

# Sources of quantized excitations via dichotomic topological cycles

Bryan Leung<sup>1,\*</sup> and Emil Prodan<sup>2,†</sup>

<sup>1</sup>*Spotify, New York, NY, USA*

<sup>2</sup>*Department of Physics, Yeshiva University, New York, NY, USA*

We demonstrate the existence of a conceptually distinct topological pumping phenomenon in 1-dimensional chains undergoing topological adiabatic cycles. Specifically, for a stack of two such chains cycled in opposite directions and coupled at one edge by a gapping potential, a quantized number of states are transferred per cycle from one chain to the other. The quantized number is determined by the bulk Chern number associated to the adiabatic cycle of a single disconnected bulk chain. The phenomenon is exemplified numerically with the Rice-Mele model. The claim is formulated using the relative index of two projections and proven using K-theoretic calculations. Possible experimental implementations with classical and quantum degrees of freedom are discussed.

Topological pumping in adiabatic cyclic dynamics is a well understood phenomenon [1]. The prototypical example is the 1-dimensional Rice-Mele lattice model [2]. When mapped in the parameter space, the model displays two energy bands except for a singular point where the model is gapless. A cyclic adiabatic driving supplies an additional variable that can be treated as a quasi-momentum, hence the dimension of the model is enhanced from 1 to 2. If the adiabatic cycle encloses the singularity, the spectral projections corresponding to the energy bands carry non-trivial Chern numbers [3], which are revealed by the chiral edge modes emerging from the bulk spectrum when the system is halved. The difference between right moving and left moving chiral modes equals the corresponding bulk Chern number.

This robust phenomenon was confirmed experimentally not long ago with ultra-cold fermionic and bosonic atoms [4, 5], even though the prediction was made forty years ago. Since then, the phenomenon has received renewed attention from the meta-material community because of the possibility of resonant spectrum engineering [6–11], of topological wave-steering [12–20], as well as of dynamic edge-to-edge pumping [21–24]. The last batch of experimental achievements are highly relevant for the present work, because they demonstrated that fast dynamic re-configurations of the meta-materials are now possible, to a level where the pumped signals do not succumb to dissipation and the effect can be revealed. This assures us that the topological effects predicted here are within the experimental reach. Only a few of these experimental works rely on the Rice-Mele model (*e.g.* [21]) and the rest actually rely on aperiodic models. The ideas we introduce here are model independent, but the Rice-Mele is used to make the presentation concrete.

A prior work by the authors [?] pointed out the existence of a conceptually distinct pumping phenomenon, which was formulated in the context of 3-dimensional condensed matter systems displaying the quantized magneto-electric effect. In this letter, we demonstrate that this pumping phenomenon also occurs in 1-dimensional systems displaying topological adia-

batic cycles, which can be handled much easier in a laboratory.

For this, let us consider the Rice-Mele Hamiltonian

$$H = \sum_n \left[ \left( \frac{1}{2} + (-1)^n \frac{\delta}{2} \right) |n\rangle\langle n+1| + (-1)^n \frac{\Delta}{2} |n\rangle\langle n| \right] + h.c. \quad (1)$$

Fig. 1a shows its spectral gap mapped as function of the parameters  $\delta$  and  $\Delta$ , together with two adiabatic paths parametrized by the circle  $\mathbb{S}^1 = \mathbb{R}/\mathbb{Z}$ , of which  $\gamma_1$  encloses the gap singularity while  $\gamma_2$  does not. The Chern number for a closed and spectrally gapped loop  $\gamma$  is

$$\text{Ch}_\gamma = i \int_{\mathbb{S}^1} d\tau \text{Tr}_L \left( P(\tau) \left[ \partial_\tau P(\tau), i[X, P(\tau)] \right] \right), \quad (2)$$

where  $P(\tau) = \chi_{(-\infty, 0]}(H(\gamma_\tau))$  is the spectral projector onto the lower energy band,  $X$  is the position operator and  $\text{Tr}_L$  is the trace per length. Throughout,  $\chi_A$  denotes the characteristic function of the set  $A$ .  $\text{Ch}_\gamma$  is written in real-space rather than  $k$ -space to convey that it is well defined in the presence of disorder [25]. The difference between  $\gamma_1$  and  $\gamma_2$  is that  $\text{Ch}_{\gamma_1} = 1$  while  $\text{Ch}_{\gamma_2} = 0$ . The expected chiral edge modes traversing the spectral bulk gap for  $\gamma_1$  are illustrated in Fig. 1(b).

We now consider a stack of two infinite Rice-Mele chains and an adiabatic cycle  $\gamma$ , but we run the adiabatic cycle in opposite directions for the two blocks, namely

$$\mathbf{H}_0(t) = \begin{pmatrix} H(\gamma_\tau) & 0 \\ 0 & H(\gamma_{-\tau}) \end{pmatrix}, \quad \tau = \frac{t}{T}, \quad (3)$$

with  $t$  the real time and  $T$  the total duration of cycle. It will be convenient to use  $T$  as the unit of time, in which case  $t$  and  $\tau$  coincide and we can use the latter throughout. Hamiltonian  $\mathbf{H}_0(\tau)$  will play the role of the bulk Hamiltonian. Throughout, our convention will be to bold all operators related to the double-chain system. Now, if one calculates the total Chern number of the lower energy band, one will find a trivial value, regardless if  $\gamma$  encloses the critical point or not. As such, one will be inclined to proclaim that all topological characteristics are lost. Our main message is that this is not the

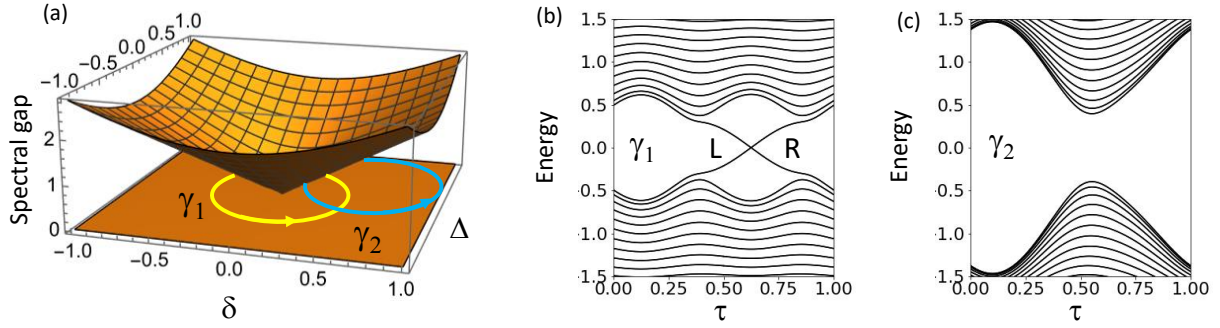


FIG. 1. (a) Spectral gap of the Hamiltonian (1) as a function of the parameters  $(\delta, \Delta)$ , together with two adiabatic cycles, of which  $\gamma_1 = (\delta = 0.3 \cos(2\pi\tau + \pi/4), \Delta = 0.3 \sin(2\pi\tau + \pi/4))$  circles and  $\gamma_2 = (\delta = 0.4 + 0.3 \cos(2\pi\tau + \pi/4), \Delta = 0.4 + 0.3 \sin(2\pi\tau + \pi/4))$  does not circle the gap singularity at  $\delta = \Delta = 0$ . The phase shift and the values of the amplitudes are chosen such that various band crossings do not overlap, which is important for the presentation but not for the results. (b,c) The energy spectrum of the Hamiltonian (1) as a function of the adiabatic parameter  $\tau$  for  $\gamma_1$  and  $\gamma_2$ , respectively. Both spectra are generated with chains of 20 sites. Two chiral modes located at opposite left (L) and right (R) ends of the chains are visible in panel (b). These chiral modes are absent for the adiabatic cycle  $\gamma_2$ .

case at all! Let us examine the spectral flows reported in Figs. 2(a,b) of the Hamiltonian (3), when it is reduced to finite-size with open boundary conditions. The results in Fig. 2a for the contour  $\gamma_2$  are not very interesting, but an opportunity presents itself for contour  $\gamma_1$  in Fig. 2b. Indeed, two opposite chiral bands spatially localized at the *same* edge intersect each other as indicated by the arrow. Then a generic edge potential hybridizes these bands and gaps the system at that edge, potentially resulting in a quantized spectral flow from the top to the bottom chain. We are cautious here because, a priori, one cannot exclude the existence of other band splittings un-doing the effect.

To exemplify that the effect is possible, we designed an edge potential that hybridizes only the two chiral bands present at the left edges, leaving the rest of the spectrum *intact*. This irrefutably proves that the transfer of quantized excitations from one chain to the other is possible. The topological character of the process, that is, its robustness against deformations of the bulk models and edge potentials, as well as inclusion of disorder, is a separate question, which will be addressed in the second part of our work. In the following computations, all Hamiltonians are assumed finite and with open boundary conditions. Now, let us consider an energy window  $\Delta E = [E_-, E_+]$  around the band crossing (see Fig. 2b) and let  $P_{\Delta E}(\tau) = \chi_{[E_-, E_+]}(H(\gamma_\tau))$  be the corresponding spectral projection of the top chain. Then our proposed edge potential takes the form

$$\mathbf{V}_{\text{edge}}(\tau) = \lambda(\tau) \begin{pmatrix} 0 & P_{\Delta E}(\tau)P_{\Delta E}(-\tau) \\ P_{\Delta E}(-\tau)P_{\Delta E}(\tau) & 0 \end{pmatrix}, \quad (4)$$

where  $\lambda(\tau)$  is a smooth on-off switch that is zero outside the small window shown in Fig. 2b centered at the crossing point. Note that  $P_{\Delta E}(\tau)$  displays discontinuities when the chiral bands cross the edges of interval  $\Delta E$ , but

those discontinuities disappear once the smooth on-off switch is included. More, the spectral projection of  $\mathbf{H}_0(\tau)$  on the interval  $\Delta E = [E_-, E_+]$ ,

$$\mathbf{Q}_{\Delta E}(\tau) := \chi_{[E_-, E_+]}(\mathbf{H}_0(\tau)) = \begin{pmatrix} P_{\Delta E}(\tau) & 0 \\ 0 & P_{\Delta E}(-\tau) \end{pmatrix}, \quad (5)$$

commutes with our specially designed edge potential and this assures us that only the states inside the spectral interval  $[E_-, E_+]$  are affected by  $\mathbf{V}_{\text{edge}}(\tau)$ .

The spectral flow of the full Hamiltonian

$$\mathbf{H}(\tau) = \mathbf{H}_0(\tau) + \mathbf{V}_{\text{edge}}(\tau), \quad \tau = t/T, \quad (6)$$

schematized in Fig. 3, is reported in Fig. 2c. As expected, the spectrum has been modified only inside the marked window, where one can clearly distinguish a splitting of the left-localized chiral bands. Outside the marked window, the two Rice-Mele chains are decoupled, hence the eigenstates have a well defined top/bottom index, which is color labeled in Fig. 2. Based on this concrete spectral flow, the following statement holds: If at  $t = 0$  one fully populates the states below the bulk spectral gap of the top chain, leaving the states of the bottom chain completely empty, then exactly one normalized state will be detected on the bottom chain after one full adiabatic cycle.

It then becomes clear that the adiabatic cycle described above acts like a valve that releases one excitation per cycle into the bottom chain. Hence, our proposed set-up supplies the design principles for on-demand sources of quantized excitations. Here are two possible laboratory implementations. The first one involves phonons. In this context, the sites of the Rice-Mele chains harbor identical mechanical resonators which are coupled as indicated by our Hamiltonian (6). This will require re-configurability but, as stressed in the beginning, this is now more or less

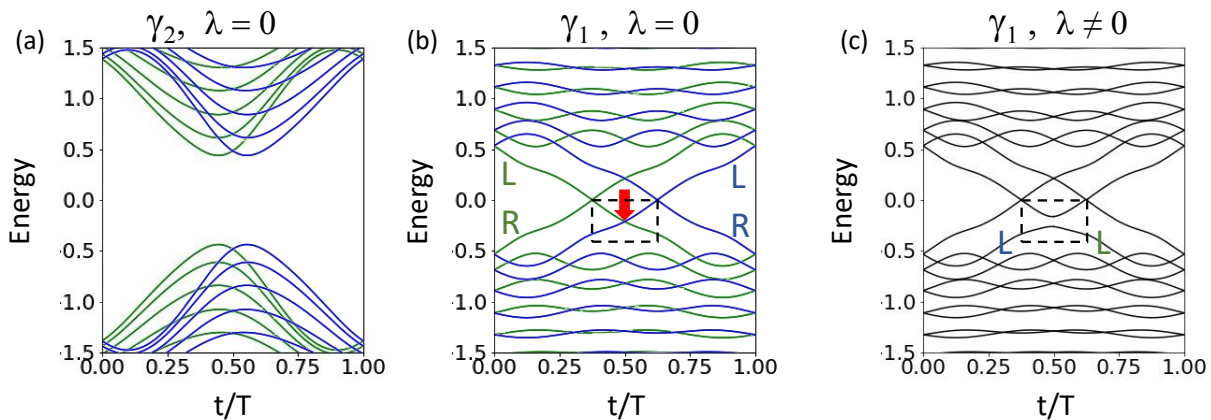


FIG. 2. Spectral flow of the Hamiltonian (3) deployed on finite-size chains with open boundary conditions, when adiabatically deformed along (a) the cycle  $\gamma_2$ , and (b) the cycle  $\gamma_1$ . (c) Same as panel (b), but for Hamiltonian (6). The labels L/R indicate the spatial localization of the chiral bands to either left (L) or right (R) edge of the system. Marked with an arrow in panel (b) is the crossing of the chiral bands localized at the right edge of the system. The window drawn with a dashed line indicates the energy and time ranges where the edge potential (4) is defined. The data is generated with finite chains containing 10 sites and  $\lambda(t)$  for panel (c) is turned up to 0.2. The blue and green color represent top and bottom states respectively.

under control. With the chains decoupled, the upper chain is excited with a broad spectrum source, such that all phonon modes below the spectral gap are uniformly excited. Then, after one turn of our proposed cycle, a *single* phonon will be detected propagating to the right on the lower mechanical chain. With electrons, the situation is more difficult because populating and de-populating energy bands is a more involved process. Still, we believe that the effect can be implemented with a half-filled virtual spin-Chern insulator. By applying a strong upward magnetic field, we can populate the up-spin states and completely depopulate the down-spin states. The magnetic field can then be abruptly turned off and the adiabatic cycle initiated. After one turn of the adiabatic cycle, one should observe a quantized spin-down excitation moving to the right. Of course, all these will take place in the background of the relaxation process back to the equilibrium state. Hence, the success of such enterprise requires the adiabatic cycle to be shorter than the relaxation time. The recent cold-atom simulations of spin-Chern insulators [26] show a level of control that we believe is sufficient for implementing and observing

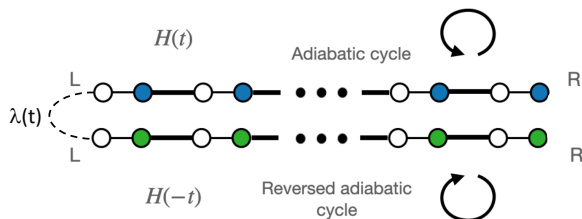


FIG. 3. Illustration of coupled Rice-Mele chains driven in opposite adiabatic cycles while connected at the left edge.

the effect proposed here.

We now address the topological character of the process. To derive the bulk-boundary correspondence, we send the right edge to  $\infty$ , hence the adiabatically cycled system is now semi-infinite. By doing so, we clear up the spectral gap of the right chiral bands and, as such, we can apply the adiabatic theorem to the lower spectrum. To distinguish between the bulk and half-space operators, we will place a hat on the latter. Hence, the Hamiltonian (6) becomes  $\widehat{H}$ . Furthermore, the operators with matrix elements decaying to zero away from the edge will carry a tilde. Hence, the potential (4) becomes  $\widetilde{V}_{\text{edge}}$ . If  $\widehat{U}_\tau$  is the physical time evolution operator, *i.e.* the unitary solution of the equation,  $i\partial_\tau \widehat{U}_\tau = T\widehat{H}(\tau)\widehat{U}_\tau$ ,  $\widehat{U}_0 = \mathbf{1}$ , then it is well-known [27] that  $\widehat{U}_\tau$  can be approximated by the adiabatic time evolution  $\widehat{U}_\tau^A$  (see Appendix 1). Then our task is to compare the projections

$$\widehat{\Pi}_0 = \begin{pmatrix} \widehat{P}(0) & 0 \\ 0 & 0 \end{pmatrix} \text{ and } \widehat{\Pi}_1^A = \widehat{U}_1^A \begin{pmatrix} \widehat{P}(0) & 0 \\ 0 & 0 \end{pmatrix} \widehat{U}_1^{A*}, \quad (7)$$

encoding the initial and final states of the two-chain system for large  $T$ . Here,  $\widehat{P}(0) = \chi_{(-\infty, 0]}(\widehat{H}(\gamma_0))$  is the spectral projection of the top chain at the beginning of the cycle.

Before we start, we want to point out the unusual character of the setting. On one hand, the bulk topology, prompted by the non-zero Chern number  $\text{Ch}_{\gamma_1}$ , exists in the  $(1+1)$ -dimensional space (one real and one virtual dimension). On the other hand, Eq. (7) compares projections on a semi-infinite quasi-one dimensional system, because time does not appear as a variable in Eq. (7). As we shall see, this comparison provides a topological invariant that is associated to the edge physics of the semi-infinite static system. Hence, our task is to connect

the bulk topology of a (1 + 1)-dimensional system with the edge topology of a 1-dimensional system, and this is a jump from a 2-dimensional system to a 0-dimensional one. Thus, we are dealing with a higher-order topological phenomenon, but we are not able to connect it with any other known mechanism of higher-order topology.

We now start the analysis. First, note that the bulk-systems, such as  $H$  or  $\mathbf{H}_0$  belong to the algebra of double-periodic operators, denoted by  $\mathcal{A}$  in the following (adding or multiplying doubly-periodic operators preserves that property). The adiabatically driven Hamiltonians, such as  $H(\gamma_\tau)$  or  $\mathbf{H}_0(\tau)$ , then belong to algebra  $\mathcal{A}^{\mathbb{S}^1}$  of maps from the circle  $\mathbb{S}^1$  to the algebra  $\mathcal{A}$ . The operators with matrix elements concentrated around the edge live in the algebra  $\widetilde{\mathcal{A}}$  (indeed, the sums and products of edge operators remain edge operators). In between  $\mathcal{A}$  and  $\widetilde{\mathcal{A}}$  is the algebra  $\widehat{\mathcal{A}}$  of half-space operators whose elements are doubly-periodic Hamiltonians with clean open boundary condition at the edge plus any element from the edge algebra:  $\widehat{A} = A|_{\text{open}} + \widetilde{V}_{\text{edge}}$ . The projections from Eq. (7) belong to  $M_2 \otimes \widehat{\mathcal{A}}$ , where  $M_N$  denotes the algebra of  $N \times N$  matrices. Two projections are said to be homotopic if they can be deformed continuously into each other without leaving the algebra they belong to. Since in condensed matter physics and meta-material science we always work with effective models, it is more appropriate to include additional trivial bands, accounting for the neglected orbitals or degrees of freedom, and allow the deformations to spill out into these additional bands. In other words, to allow the deformations to take place in  $M_\infty \otimes \widehat{\mathcal{A}}$ , where  $M_\infty$  is the algebra of arbitrary rank matrices. In this case, one talks about stable homotopy and the K-theoretic group  $K_0(\widehat{\mathcal{A}})$  classifies the projections with respect to this equivalence relation. Note that the stably-homotopic class  $[\Pi]_0$  of a projection from  $M_\infty \otimes \widehat{\mathcal{A}}$  is the *complete* topological invariant associated to  $\Pi$  [28].

A K-theoretic calculation detailed in Appendix 3 shows that the difference

$$\left[\widehat{\Pi}_1^A\right]_0 - \left[\widehat{\Pi}_0\right]_0 \quad (8)$$

actually lands in the K-theoretic group  $K_0(\widetilde{\mathcal{A}})$  of the edge algebra. Among other things, this implies that the difference between the projections from Eq. (7) belongs to the simple algebra  $M_\infty$ . It is an important detail because it enables us to connect to the work by Avron, Seiler and Simon on the relative index of projections [29–31]. Their original application was on a comparison between the Fermi projections of 2-dimensional systems with and without Dirac fluxes piercing the plane of the sample. The mathematical concept supplied a rigorous framework for Laughlin’s pumping argument for the integer quantum Hall effect [32]. In our context, the relative index of the projections (7) is a numerical topological

invariant derived from the complete topological invariant (8), which measures their relative dimension.

We are now ready to state our main result: For any edge potential  $\widetilde{V}_{\text{edge}}(\tau)$  that gaps the spectrum for the entire duration of the cycle and vanishes for  $\tau$  in small interval  $[-\epsilon, \epsilon]$  around the initial/final points, we have

$$\text{Ind}(\widehat{\Pi}_1^A, \widehat{\Pi}_0) = \text{Ch}_{\gamma}, \quad (9)$$

where on the right is the Chern number (2) associated to a single Rice-Mele chain. In fact, in Appendix 3, we derive a relation between the complete invariant (8) and the complete topological invariant  $[\tau \mapsto P(\tau)]_0 \in K_0(\mathcal{A}^{\mathbb{S}^1})$ , which carries the Chern number  $\text{Ch}_\gamma$ . It takes the form

$$\left[\widehat{\Pi}_1^A\right]_0 - \left[\widehat{\Pi}_0\right]_0 = \left(\text{Ind} \circ \theta^{-1}\right)\left([\tau \mapsto P(\tau)]_0\right), \quad (10)$$

where  $\theta$  is the map appearing in the Bott periodicity theorem and  $\text{Ind}$  is the K-theoretic connecting map associated to the exact sequence of algebras  $\widetilde{\mathcal{A}} \twoheadrightarrow \widehat{\mathcal{A}} \twoheadrightarrow \mathcal{A}$  (see Appendix 2 and [33] for more details). Small disorder is automatically included in these calculations.

In terms of the spectral flows reported in Fig. 2, we can interpret these predictions in the following way. Note that for  $\gamma_1$  in Fig. 2c, there is an additional swap between an occupied and an un-occupied state for the top chain. But this swap takes place at the right edge and, when the right edge is sent to  $\infty$ , an observer operating at the origin will not be able to detect it. To this observer, it will appear that one state below the gap has been populated during the adiabatic cycle, without de-populating any other state. As such, this newly populated state must reside on the bottom chain. In contrast, for  $\gamma_2$ , while a connecting edge potential can still hybridize top and bottom non-chiral edge bands, there will be an equal number of top-bottom and bottom-up swaps of states, all taking place at the left edge. Hence, the observer will not detect any net increase in the population of the states. Furthermore, the non-topological edge bands are unstable and can disappear under deformations.

In conclusion, we have discovered a distinct pumping process which can lead to new applications of topology in condensed matter physics and meta-material science. Based on our rigorous statements, we can assure the experimental scientists that no fine-tuning of the edge potential is required to achieve the quantized effect, because a generic edge potential will typically gap the spectrum. Furthermore, the effect is robust against deformations and inherent small design imperfections.

E. P. acknowledges support from the National Science Foundation grants DMR-1823800 and CMMI-2131760.

---

\* bleung@spotify.com

- <sup>†</sup> prodan@yu.edu
- [1] D. J. Thouless. *Quantization of particle transport*, Phys. Rev. B, 27:6083–6087, (1983).
  - [2] M. J. Rice and E. J. Mele. *Elementary excitations of a linearly conjugated diatomic polymer*, Phys. Rev. Lett., 49:1455–1459, (1982).
  - [3] D. Xiao, M.-C. Chang, Q. Niu, *Berry phase effects on electronic properties*, Rev. Mod. Phys. **82**, 1959 (2010).
  - [4] S. Nakajima, T. Tomita, S. Taie, T. Ichinose, H. Ozawa, L. Wang, M. Troyer, and Y. Takahashi. *Topological Thouless pumping of ultracold fermions*, Nature Phys, **12**, 296–300 (2016).
  - [5] M. Lohse, C. Schweizer, O. Zilberberg, M. Aidelsburger, and I. Bloch. *A Thouless quantum pump with ultracold bosonic atoms in an optical superlattice*, Nature Phys. **12**, 350–354 (2016).
  - [6] D. J. Apigo, K. Qian, C. Prodan, E. Prodan, *Topological edge modes by smart patterning*, Phys. Rev. Materials **2**, 124203 (2018).
  - [7] D. J. Apigo, W. Cheng, K. F. Dobiszewski, E. Prodan, C. Prodan, *Observation of topological edge modes in a quasi-periodic acoustic waveguide*, Phys. Rev. Lett. **122**, 095501 (2019).
  - [8] X. Ni, K. Chen, M. Weiner, D. J. Apigo, C. Prodan, A. Alù, E. Prodan, A. B. Khanikaev, *Observation of Hofstadter butterfly and topological edge states in reconfigurable quasi-periodic acoustic crystals*, Commun. Physics **2**, 55 (2019).
  - [9] H. U. Voss, D. J. Ballon, *Topological modes in radiofrequency resonator arrays*, Phys. Lett. A **384**, 126177 (2020).
  - [10] M. Hafezi, S. Mittal, J. Fan, A. Migdall, J. M. Taylor, *Imaging topological edge states in silicon photonics*, Nat. Photonics **7**, 1001 (2013).
  - [11] Y. Xia, A. Erturk, M. Ruzzene, Massimo, *Topological edge states in quasiperiodic locally resonant metastructures*, Phys. Lett. A **13**, 014023 (2020).
  - [12] Y. E. Kraus, Y. Lahini, Z. Ringel, M. Verbin, O. Zilberberg, *Topological states and adiabatic pumping in quasicrystals*, Phys. Rev. Lett. **109**, 106402 (2012).
  - [13] M. Verbin, O. Zilberberg, Y. Lahini, Y. Kraus, Y. Silberberg, *Topological pumping over a photonic Fibonacci quasicrystal*, Phys. Rev. B **91**, 064201 (2015).
  - [14] M. I. N. Rosa, R. K. Pal, J. R. F. Arruda, and M. Ruzzene, *Edge states and topological pumping in spatially modulated elastic lattices*, Phys. Rev. Lett. **123**, 034301 (2019).
  - [15] E. Riva, M. I. N. Rosa, and M. Ruzzene, *Edge states and topological pumping in stiffness-modulated elastic plates*, Phys. Rev. B **101**, 094307 (2020).
  - [16] Y. Shen, Y. Peng, D. Zhao, X. Chen, J. Zhu, and X. Zhu, *One-way localized adiabatic passage in an acoustic system*, Phys. Rev. Lett. **122**, 094501 (2019).
  - [17] O. Zilberberg, S. Huang, J. Guglielmon, M. Wang, K. Chen, Y. E. Kraus, M. C. Rechtsman, *Photonic topological pumping through the edges of a dynamical four-dimensional quantum Hall system*, Nature (London) **553**, 59 (2018).
  - [18] E. Lustig, S. Weimann, Y. Plotnik, Y. Lumer, M. A. Bandres, A. Szameit, M. Segev, *Photonic topological insulator in synthetic dimensions*, Nature (London) **567**, 356 (2019).
  - [19] W. Cheng, E. Prodan, C. Prodan, *Revealing the boundary Weyl physics of the four-dimensional Hall effect via phason engineering in metamaterials*, Phys. Rev. Applied **16**, 044032 (2021).
  - [20] H. Chen, H. Zhang, Q. Wu, Y. Huang, H. Nguyen<sup>1</sup>, E. Prodan, X. Zhou, G. Huang, *Creating synthetic spaces for higher-order topological sound transport*, Nature Comm. **12**, 5028 (2021).
  - [21] I. H. Grinberg, M. Lin, C. Harris, W. A. Benalcazar, C. W. Peterson, T. L. Hughes, and G. Bahl, *Robust temporal pumping in a magneto-mechanical topological insulator*, Nat. Commun. **11**, 974 (2020).
  - [22] Y. Xia, E. Riva, M. I. N. Rosa, G. Cazzulani, A. Erturk, F. Braghin, M. Ruzzene, *Experimental observation of temporal pumping in electro-mechanical waveguides*, Phys. Rev. Lett. **126**, 095501 (2021).
  - [23] W. Cheng, E. Prodan, C. Prodan, *Experimental demonstration of dynamic topological pumping across incommensurate bilayered acoustic metamaterials*, Phys. Rev. Lett. **125**, 224301 (2020).
  - [24] X Xu *et al*, *Physical observation of a robust acoustic pumping in waveguides with dynamic boundary*, Phys. Rev. Lett. **125**, 253901 (2020).
  - [25] J. Bellisard, A. van Elst, H. Schulz-Baldes, *The noncommutative geometry of the quantum Hall effect*, J. Math. Phys. **35**, 5373–451 (1994).
  - [26] Q-X. Lv *et al*, *Measurement of spin Chern numbers in quantum simulated topological insulators*, Phys. Rev. Lett. **127**, 136802 (2021).
  - [27] J. E. Avron, R. Seiler, L. G. Yaffe, *Adiabatic Theorems and Applications to the Quantum Hall Effect*, Commun. Math. Phys. **110**, 33–49 (1987).
  - [28] A topological invariant is called complete if it determines the classification entirely.
  - [29] J. Avron, R. Seiler, B. Simon, *The quantum Hall effect and the relative index for projections*, Phys. Rev. Lett. **65**, 2185–2188 (1990).
  - [30] J. Avron, R. Seiler, B. Simon, *Charge deficiency, charge transport and comparison of dimensions*, Commun. Math. Phys. **159**, 399–422 (1994).
  - [31] J. Avron, R. Seiler, B. Simon, *The index of a pair of projections*, J. Funct. Anal. **120**, 220–237 (1994).
  - [32] R. Laughlin, in *The quantum Hall effect*, edited by R. E. Prange and S. M. Garvin, (Springer-Verlag, Berlin, 1987).
  - [33] M. Rordam, F. Larsen, N. Laustsen, *An Introduction to K-Theory for  $C^*$ -Algebras* (Cambridge University, Cambridge Press, 2000).

## APPENDIX 1: ADIABATIC THEOREM AND MONODROMIES OF PROJECTIONS

The physical time evolution under the full Hamiltonian  $\widehat{H}(t)$  is supplied by the time propagator  $\widehat{U}_t$ , which is the unique unitary solution of the Schrödinger equation

$$i\partial_t \widehat{U}_t = \widehat{H}(t)\widehat{U}_t, \quad \widehat{U}_0 = \mathbf{1}. \quad (11)$$

If one passes to the scaled time  $\tau = t/T \in [0, 1]$  using the period  $T$  of the cycle, the equation becomes

$$i\partial_\tau \widehat{U}_\tau = T\widehat{H}(\gamma_\tau)\widehat{U}_\tau, \quad \widehat{U}_0 = \mathbf{1}. \quad (12)$$

The adiabatic time propagator  $\widehat{U}_\tau^A$  á la Kato [1] is the unique unitary solution of the following equation

$$i\partial_\tau \widehat{U}_\tau^A = (T\widehat{H}(\gamma_\tau) + i[\partial_\tau \widehat{Q}(\tau), \widehat{Q}(\tau)])\widehat{U}_\tau^A \quad (13)$$

with the initial condition  $\widehat{U}_0^A = \mathbf{1}$ , where

$$\widehat{Q}(\tau) = \chi_{(-\infty, E_c]}(\widehat{H}(\gamma_\tau)) \quad (14)$$

is the spectral projection of  $\widehat{H}(\gamma_\tau)$  onto the spectrum below the spectral gap.

The adiabatic theorem states that [2][p. 42]

$$\widehat{U}_\tau^* \widehat{U}_\tau^A = I + \mathcal{O}(1/T) \quad \forall \tau \in [0, 1]. \quad (15)$$

This, in turn, assures us that

$$\widehat{U}_\tau \widehat{\Pi}_0 \widehat{U}_\tau^* - \widehat{U}_\tau^A \widehat{\Pi}_0 \widehat{U}_\tau^{A*} = \mathcal{O}(1/T), \quad (16)$$

which justifies the use of  $\widehat{\Pi}_\tau^A$  in our statements. The hallmark property of  $\widehat{U}_\tau^A$  is that

$$\widehat{U}_\tau^A \widehat{Q}(0) \widehat{U}_\tau^{A*} = \widehat{Q}(\tau). \quad (17)$$

As such,

$$\widehat{W}_\tau := \widehat{U}_\tau^A \widehat{Q}(0) \quad (18)$$

supplies a monodromy of  $\widehat{Q}(\tau)$ , *i.e.* a partial isometry with the properties

$$\widehat{W}_\tau^* \widehat{W}_\tau = \widehat{Q}(0), \quad \widehat{W}_\tau \widehat{W}_\tau^* = \widehat{Q}(\tau). \quad (19)$$

In particular,

$$\widehat{W}_1^* \widehat{W}_1 = \widehat{Q}(0), \quad \widehat{W}_1 \widehat{W}_1^* = \widehat{Q}(1) = \widehat{Q}(0), \quad (20)$$

and

$$\widehat{W}_1 + \mathbf{1} - \widehat{Q}(0) \quad (21)$$

is a unitary operator from the algebra  $\widehat{\mathcal{A}}$ .

## APPENDIX 2: ALGEBRAS OF OBSERVABLES AND THEIR RELATIONS

The algebras of physical observables  $\mathcal{A}$ ,  $\widehat{\mathcal{A}}$ ,  $\widetilde{\mathcal{A}}$  and  $\mathcal{A}^{\mathbb{S}^1}$  introduced in the main text can be connected via exact sequences. One well-known short exact sequence of  $C^*$ -algebras is [3]

$$0 \rightarrow \widetilde{\mathcal{A}} \xrightarrow{i} \widehat{\mathcal{A}} \xrightarrow{\text{ev}} \mathcal{A} \rightarrow 0 \quad (22)$$

where  $i$  is the inclusion map and the evaluation map is

$$\text{ev}(A|_{\text{open}} + \widetilde{V}_{\text{edge}}) = A \quad (23)$$

Another exact sequence relates to the adiabatic cycle

$$0 \rightarrow \mathcal{S}\mathcal{A} \xrightarrow{i} \mathcal{A}^{\mathbb{S}^1} \xrightarrow{\text{ev}} \mathcal{A} \rightarrow 0 \quad (24)$$

where  $\mathcal{S}\mathcal{A}$  denotes the suspension of the algebra  $\mathcal{A}$ , that is, the ideal generated by the elements  $A(\tau) \in \mathcal{A}^{\mathbb{S}^1}$  with  $A(0) = 0$ . The evaluation map above is  $\text{ev}(A(\tau)) = A(0)$ . Similar sequences exist for the suspensions of the algebras  $\widehat{\mathcal{A}}$  as well as  $\widetilde{\mathcal{A}}$ . They can all be combined in the following commutative diagram [4]:

$$\begin{array}{ccccccc}
 & & 0 & & 0 & & 0 \\
 & & \uparrow & & \uparrow & & \uparrow \\
 0 & \longrightarrow & \mathcal{S}\mathcal{A} & \xrightarrow{i} & \mathcal{A}^{\mathbb{S}^1} & \xrightarrow{\text{ev}} & \mathcal{A} \longrightarrow 0 \\
 & & \uparrow & & \uparrow & & \uparrow \\
 0 & \longrightarrow & \mathcal{S}\widehat{\mathcal{A}} & \xrightarrow{i} & \widehat{\mathcal{A}}^{\mathbb{S}^1} & \xrightarrow{\text{ev}} & \widehat{\mathcal{A}} \longrightarrow 0 \\
 & & \uparrow & & \uparrow & & \uparrow \\
 0 & \longrightarrow & \mathcal{S}\widetilde{\mathcal{A}} & \xrightarrow{i} & \widetilde{\mathcal{A}}^{\mathbb{S}^1} & \xrightarrow{\text{ev}} & \widetilde{\mathcal{A}} \longrightarrow 0 \\
 & & \uparrow & & \uparrow & & \uparrow \\
 & & 0 & & 0 & & 0
 \end{array}$$

We point out that the bulk adiabatic process of one chain takes place inside the algebra located in the upper-left corner of the diagram. The relative index of projections mentioned in the main text is associated to the algebra of edge observables, which is located at the bottom-right corner of the diagram.

Every long exact sequence of  $C^*$ -algebras

$$0 \rightarrow \mathcal{J} \xrightarrow{i} \mathcal{B} \xrightarrow{\text{ev}} \mathcal{B}/\mathcal{J} \rightarrow 0 \quad (25)$$

induces a six-term exact sequence among the K-theories [5], which is central to the rigorous derivations of the bulk-boundary correspondence principles [6]:

$$\begin{array}{ccccc}
K_0(\mathcal{J}) & \xrightarrow{i_*} & K_0(\mathcal{B}) & \xrightarrow{\text{ev}_*} & K_0(\mathcal{B}/\mathcal{J}) \\
\uparrow \text{Ind} & & & & \downarrow \text{Exp} \\
K_1(\mathcal{B}/\mathcal{J}) & \xleftarrow{\text{ev}_*} & K_1(\mathcal{B}) & \xleftarrow{i_*} & K_1(\mathcal{J})
\end{array} \quad (26)$$

If the exact sequence is the particular sequence from Eq. 24, then, traditionally, the Ind and Exp maps are denoted by  $\theta$  and  $\beta$ . These maps play a central role in Bott's periodicity theorem [5].

By applying this principle to the commuting diagram from above, we produce the following sequence

$$K_0(\mathcal{S}\mathcal{A}) \xrightarrow{\theta^{-1}} K_1(\mathcal{A}) \xrightarrow{\text{Ind}} K_0(\widetilde{\mathcal{A}}) \quad (27)$$

which will be our main tool for deriving the bulk-boundary correspondence in Appendix 3. This diagram connects the complete topological invariants of the bulk adiabatic process of a single chain and of its edge physics.

Let us point out that any projection  $\tau \mapsto P(\tau)$  from  $\mathcal{A}^{\mathbb{S}^1}$  generates a canonical element from  $K_0(\mathcal{S}\mathcal{A})$  via

$$[\tau \mapsto P(\tau)]_0 - [\tau \mapsto P(0)]_0 \quad (28)$$

This will be tacitly assumed throughout.

Let us also point out that all the algebras mentioned above can be promoted to include weak disorder. All the statements made below remain valid for this more general context (see [4] for details).

### APPENDIX 3: BULK-BOUNDARY CORRESPONDENCE AND THE EDGE INDEX

Here we provide the proof to the statement from Eq. (10), which follows closely the proof of Prop 6.3 in [4]. First, the inverse map  $\theta^{-1} : K_0(\mathcal{S}\mathcal{A}) \rightarrow K_1(\mathcal{A})$  for the class of

$$P(\tau) = \chi_{(-\infty, 0]}(H(\gamma_\tau)), \quad \tau \in \mathbb{S}^1, \quad (29)$$

in  $K_0(\mathcal{S}\mathcal{A})$  was computed in Proposition 4.1.8 of [3]. It is given by

$$\theta^{-1}([\tau \mapsto P(\tau)]_0) = [V_1 + 1 - P(0)]_1, \quad (30)$$

where  $V_\tau$  is the monodromy of  $P(\tau)$ , *i.e.*

$$V_\tau = U_\tau^A P(0) \quad (31)$$

with  $U_\tau^A$  the unitary solution of the adiabatic time evolution equation

$$i\partial_\tau U_\tau^A = (TH(\gamma_\tau) + i[\partial_\tau P(\tau), P(\tau)])U_\tau^A, \quad U_0^A = I. \quad (32)$$

Then our next task is to compute

$$\text{Ind}([V_1 + 1 - P(0)]_1), \quad (33)$$

where Ind is the index map associated to the sequence (22).

The standard picture of the index map [5] states that, for any unitary operator  $U \in \mathcal{A}$ ,

$$\text{Ind}([U]_1) = \left[ \widehat{U} \begin{pmatrix} 1 & 0 \\ 0 & 0 \end{pmatrix} \widehat{U}^* \right]_0 - \left[ \begin{pmatrix} 1 & 0 \\ 0 & 0 \end{pmatrix} \right]_0, \quad (34)$$

where  $\widehat{U}$  is a lift of the unitary operator  $\begin{pmatrix} U & 0 \\ 0 & U^* \end{pmatrix}$  to the algebra  $M_2 \otimes \widehat{\mathcal{A}}$ , namely

$$\text{ev}(\widehat{U}) = \begin{pmatrix} U & 0 \\ 0 & U^* \end{pmatrix}. \quad (35)$$

The key observation is that, if  $U$  is the unitary  $V_1 + 1 - P(0)$ , then  $\widehat{W}_1 + 1 - \widehat{Q}(0)$  from Eq. (21) supplies such a lift [?]. Indeed, if we apply the algebra homomorphism  $\text{ev}$  to Eq. (13), all edge operators are sent to zero and, as such, we obtain two copies of Eq. (32), of which one is ran backwards in time. Therefore,

$$\text{ev}(\widehat{W}_1) = \begin{pmatrix} V_1 & 0 \\ 0 & V_1^* \end{pmatrix}. \quad (36)$$

Furthermore,

$$\text{ev}(\widehat{Q}(0)) = \begin{pmatrix} P(0) & 0 \\ 0 & P(0) \end{pmatrix}. \quad (37)$$

Then

$$\begin{aligned}
& (\text{Ind} \circ \theta^{-1})([\tau \mapsto P(\tau)]_0) = \\
& \left[ (\widehat{W}_1 + 1 - \widehat{Q}(0)) \begin{pmatrix} 1 & 0 \\ 0 & 0 \end{pmatrix} (\widehat{W}_1 + 1 - \widehat{Q}(0))^* \right]_0 - \left[ \begin{pmatrix} 1 & 0 \\ 0 & 0 \end{pmatrix} \right]_0.
\end{aligned} \quad (38)$$

Since we assume that  $\widetilde{V}_{\text{edge}}(0) = 0$ , the following simplification occurs:

$$\widehat{Q}(0) = \begin{pmatrix} \widehat{P}(0) & 0 \\ 0 & \widehat{P}(0) \end{pmatrix}. \quad (39)$$

Hence,  $\mathbf{1} - \widehat{Q}(0)$  commutes with  $\begin{pmatrix} 1 & 0 \\ 0 & 0 \end{pmatrix}$ . Additionally, we have the relation  $\widehat{W}_1(\mathbf{1} - \widehat{Q}(0)) = 0$ . We reach the conclusion

$$(\text{Ind} \circ \theta^{-1})([\tau \mapsto P(\tau)]_0) = [\widehat{\Pi}_1^A]_0 - [\widehat{\Pi}_0]_0, \quad (40)$$

where

$$\widehat{\Pi}_1^A = \widehat{U}_1^A \begin{pmatrix} \widehat{P}(0) & 0 \\ 0 & 0 \end{pmatrix} \widehat{U}_1^{A*} \quad \text{and} \quad \widehat{\Pi}_0 = \begin{pmatrix} \widehat{P}(0) & 0 \\ 0 & 0 \end{pmatrix}, \quad (41)$$

as claimed in the main text.

Regarding the relative index of the projections, we first note that, due to Eq. (36),

$$\text{ev}(\widehat{\Pi}_1^A - \widehat{\Pi}_0) = 0, \quad (42)$$

which assures us that  $\widehat{\Pi}_1^A - \widehat{\Pi}_0 \in \widetilde{\mathcal{A}} \simeq M_\infty$  (this is a special feature of 1-dimensional systems). Then the spectrum of the self-adjoint operator  $\widehat{\Pi}_1^A - \widehat{\Pi}_0$  is discrete (except at the origin) and the possible eigenvalues  $\pm 1$  have finite degeneracies. Furthermore, there exists a unitary element  $K$  from the algebra  $\mathbb{C} \cdot I \oplus M_\infty$  such that

$$K \widehat{\Pi}_1^A K^* - \widehat{\Pi}_0 = P_{+1} - P_{-1}, \quad (43)$$

where  $P_{\pm 1}$  are the spectral projections of  $\widehat{\Pi}_1^A - \widehat{\Pi}_0$  onto  $\pm 1$ . The relative index is then [7]

$$\text{Ind}(\widehat{\Pi}_1^A, \widehat{\Pi}_0) = \text{rank } P_{+1} - \text{rank } P_{-1}. \quad (44)$$

Eq. (43) also assures us that

$$\left[ \widehat{\Pi}_1^A \right]_0 - \left[ \widehat{\Pi}_0 \right]_0 = \left[ P_{+1} \right]_0 - \left[ P_{-1} \right]_0, \quad (45)$$

as elements of  $K_0(\widetilde{\mathcal{A}})$ , hence Eq. (40) can be written as

$$\left( \text{Ind} \circ \theta^{-1} \right) \left( [\tau \mapsto P(\tau)]_0 \right) = \left[ P_{+1} \right]_0 - \left[ P_{-1} \right]_0. \quad (46)$$

By applying the standard trace, on the right side we get the relative index, while on the left side we get the Chern number of  $[\tau \mapsto P(\tau)]$ . The latter follows from the cyclic cocycle pairings relative to the connecting maps, worked out in details in [3][Sec. 5.5].

---

\* bleung@spotify.com

† prodan@yu.edu

- [1] T. Kato, *On the adiabatic theorem of quantum mechanics*, J. Phys. Soc. Japan 5, 435-439, (1950).
- [2] J. E. Avron, R. Seiler, L. G. Yaffe, *Adiabatic Theorems and Applications to the Quantum Hall Effect*, Commun. Math. Phys. 110, 33-49 (1987).
- [3] E. Prodan, H. Schulz-Baldes, *Bulk and boundary invariants for complex topological insulators: From K-theory to physics*, (Springer, Berlin, 2016).
- [4] B. Leung, E. Prodan *Bulk-boundary correspondence for topological insulators with quantized magneto-electric effect*, J. Phys. A: Math. Theor. 53, 205203 (2020).
- [5] M. Rordam, F. Larsen, N. Laustsen, *An Introduction to K-theory for C\*-algebras*, Cambridge University Press, Cambridge, (2000).
- [6] J. Kellendonk, T. Richter, H. Schulz-Baldes: *Edge current channels and Chern numbers in the integer quantum Hall effect*, Rev. Math. Phys. 14, 87-119 (2002).
- [7] J. Avron, R. Seiler, B. Simon, *The quantum Hall effect and the relative index for projections*, Phys. Rev. Lett. 65, 2185-2188 (1990).